Effects of fluctuating energy input on the small scales in turbulence

Chen-Chi Chien, Daniel B. Blum and Greg A. Voth†

Department of Physics, Wesleyan University, Middletown, Connecticut 06459, USA

In the standard cascade picture of three-dimensional turbulent fluid flows, energy is input at a constant rate at large scales. Energy is then transferred to smaller scales by an intermittent process that has been the focus of a vast literature. However, the energy input at large scales is not constant in most real turbulent flows. We explore the signatures of these fluctuations of large-scale energy input on small-scale turbulence statistics. Measurements were made in a flow between oscillating grids, with R_λ up to 262, in which temporal variations in the large-scale energy input can be introduced by modulating the oscillating grid frequency. We find that the Kolmogorov constant for second-order longitudinal structure functions depends on the magnitude of the fluctuations in the large-scale energy input. We can quantitatively predict the measured change with a model based on Kolmogorov's refined similarity theory. The effects of fluctuations of the energy input can also be observed using structure functions conditioned on the instantaneous large-scale velocity. A linear parametrization using the curvature of the conditional structure functions provides a fairly good match with the measured changes in the Kolmogorov constant. Conditional structure functions are found to provide a more sensitive measure of the presence of fluctuations in the large-scale energy input than inertial range scaling coefficients.

Key words: homogeneous turbulence, intermittency, turbulent flows

1. Introduction

One of the earliest recognitions of the importance of fluctuations in the energy dissipation rate in turbulence can be found in a footnote by Landau in the 1944 Russian edition of the textbook on fluid mechanics (Landau & Lifschitz 1944). The footnote explains that universal formulas for the small scales of structure functions do not exist because the energy dissipation rate will fluctuate on long time scales, and these fluctuations will be different in different flows. Frisch (1995) provides an extended discussion of the footnote. In the refined similarity theory by Kolmogorov (1962) and Obukhov (1962), this insight on universality is extended to include fluctuations that result from the random character of the transfer of energy between scales, which is often called internal intermittency. Kolmogorov (1962) gives Landau credit for recognizing the importance of internal intermittency. However, this credit seems to be somewhat misplaced since the available published text by Landau observes only that large-scale fluctuations in the energy dissipation will destroy

† Email address for correspondence: gvoth@wesleyan.edu

universality of the small scales (Frisch 1995; Mouri *et al.* 2006). A few years after
the footnote comment, Batchelor & Townsend (1949) provided experimental evidence
of the existence of internal intermittency. During the intensive effort to understand
internal intermittency over the past 60 years, the direct application of Landau's insight
about the importance of large-scale fluctuations has often been obscured.

   The refined similarity theory by Kolmogorov (1962) and Obukhov (1962) proposed
that in the inertial range the moments of velocity differences between two points
are universal functions when they are conditioned on the locally averaged value of
the energy dissipation rate, ε_r, defined as the instantaneous energy dissipation rate
averaged over a sphere of radius r. For simplicity we will consider the longitudinal
component of the velocity differences, $\Delta_r u$. The conditional moments are

$$\langle (\Delta_r u)^p | \varepsilon_r \rangle = C_p (\varepsilon_r r)^{p/3}, \tag{1.1}$$

where C_p are universal constants (Pope 2000). Averaging this expression over a
distribution of ε_r yields

$$\langle (\Delta_r u)^p \rangle = C_p \langle \varepsilon_r^{p/3} \rangle r^{p/3} = C_p \frac{\langle \varepsilon_r^{p/3} \rangle}{\varepsilon^{p/3}} (\varepsilon r)^{p/3}, \tag{1.2}$$

where $\varepsilon = \langle \varepsilon_r \rangle$ is the mean energy dissipation rate. Since the moments of ε_r depend on
r, this means that the inertial range scaling law is modified by internal intermittency.
Kolmogorov proposed that the fluctuations of ε_r could be described with a power law
scaling,

$$\frac{\langle \varepsilon_r^p \rangle}{\varepsilon^p} \propto \left(\frac{L}{r} \right)^{\xi_p}, \tag{1.3}$$

where L is a length characterizing the energy input scale. In Kolmogorov (1962), a
log-normal model was used to relate ξ_p for all p to $\xi_2 = \mu$, which is commonly called
the intermittency exponent. An extensive literature has explored the r dependence of
statistics of ε_r in order to understand anomalous scaling exponents in the inertial range
(Sreenivasan & Antonia 1997).

   However, the effects of fluctuations in the energy dissipation rate due to the large
scales has been given much less attention, even though this is the direct application
of Landau's original comment. Kolmogorov did state that the coefficients in the
scaling law should not be universal, presumably because he recognized that large-
scale fluctuations would not be universal (Kolmogorov 1962). Monin & Yaglom (1971)
provide a simple model at the beginning of their section titled 'refined treatment of the
local structure of turbulence, taking into account fluctuations in the dissipation rate'.
An extended presentation of this model is in the textbook by Davidson (2004). They
consider averaging together equal numbers of samples from two different turbulent
states: state 1 with energy dissipation rate $\varepsilon_1 = (1 + \gamma)\langle \varepsilon \rangle$ and another state 2 with
$\varepsilon_2 = (1 - \gamma)\langle \varepsilon \rangle$. Here $\langle \varepsilon \rangle$ is the mean energy dissipation rate and γ is a measure of
the difference in energy dissipation between the two states. Then (1.2) implies that
a measured second-order structure function in the inertial range averaged over equal
contributions from each state would be

$$\langle (\Delta_r u)^2 \rangle = \frac{C_2}{2} \left[(1 + \gamma)^{2/3} + (1 - \gamma)^{2/3} \right] (\varepsilon r)^{2/3}. \tag{1.4}$$

So the large-scale fluctuations in the energy dissipation are predicted to change the
coefficient of the inertial range scaling law without changing the power law scaling. In

this model, γ must be less than or equal to one, so the coefficient of the second-order structure function can decrease to as low as $C_2/2^{1/3} \approx 0.794 C_2$ for the case $\gamma = 1$ where there is no energy injection in state 2.

This model is easily extended to the case where samples are included from state 1 with probability β and from state 2 with probability $1 - \beta$. Now the energy dissipation rates are $\varepsilon_1 = (1 + (1 - \beta)\gamma/\beta)\langle\varepsilon\rangle$ and $\varepsilon_2 = (1 - \gamma)\langle\varepsilon\rangle$. For this extended model, the measured structure function of order p would be

$$\langle(\Delta_r u)^p\rangle = \kappa(\beta, \gamma) C_p \left(\langle\varepsilon\rangle r\right)^{p/3}, \tag{1.5}$$

where the correction factor of the coefficient is

$$\kappa(\beta, \gamma) = \left[\beta\left(1 + \frac{1-\beta}{\beta}\gamma\right)^{p/3} + (1 - \beta)(1 - \gamma)^{p/3}\right]. \tag{1.6}$$

In the limiting case $\gamma = 1$ and $\beta \to 0$, the coefficient for $p = 2$ goes to zero, and the coefficients for $p > 3$ go to infinity, so the effects of large-scale fluctuations on the small-scale statistics can be very large. In this limiting case, the flow consists of brief pulses of large energy input between long periods of no energy input.

In both Monin & Yaglom (1971) and Davidson (2004), the presentation of the model in (1.4) is followed by the observation that in typical situations this effect is not large. Figure 1 shows a contour plot of the correction factor for $p = 2$ in (1.6) as a function of the fluctuations in the energy input, γ, and the fraction of the time spent in the high energy input state, or duty cycle, β. The observation that the correction is not large in most cases is justified since the correction is less than 2.4 % for half of the parameter space for $p = 2$. However, the correction can be very large in some flows. There is always a divergence for $\gamma = 1$ and $\beta \to 0$, and for large p, the correction is larger. Although this two-state model is a simple idealization, we will show that it provides a reasonably good description of some of our data.

In real flows, the energy dissipation rate and ε_r have continuous distributions. In the continuous case, (1.2) can be used to predict the behaviour of structure functions, but there are now contributions to the distribution of ε_r from both internal intermittency and fluctuations in the energy input. In particular, ε_r for $r \geqslant L$ has a distribution which is determined not by cascade processes but by the mechanisms creating the turbulence. For the case of second-order structure functions where internal intermittency has a very small effect, we can estimate the fluctuations in the energy input and use this to predict the coefficients of the scaling law. If the mean square velocity, $3U^2 = \langle u_i u_i\rangle$, and the energy input length scale, L, are defined using ensemble averages, then they can be considered to be time-dependent. In this case, $\varepsilon \propto U^3/L$ provides an estimate of the instantaneous energy dissipation rate. If time averages of this dissipation rate are then used in (1.2), we obtain

$$\langle(\Delta_r u)^p\rangle = C_p \frac{\langle(U^3/L)^{p/3}\rangle}{\langle U^3/L\rangle^{p/3}} (\varepsilon r)^{p/3}. \tag{1.7}$$

If L has a weak dependence on the variations in the energy input, this simplifies to

$$\langle(\Delta_r u)^p\rangle = C_p \frac{\langle U^p\rangle}{\langle U^3\rangle^{p/3}} (\varepsilon r)^{p/3}. \tag{1.8}$$

If internal intermittency is important, then the effects of both fluctuations in the energy input and fluctuations in the energy transfer might be captured using the
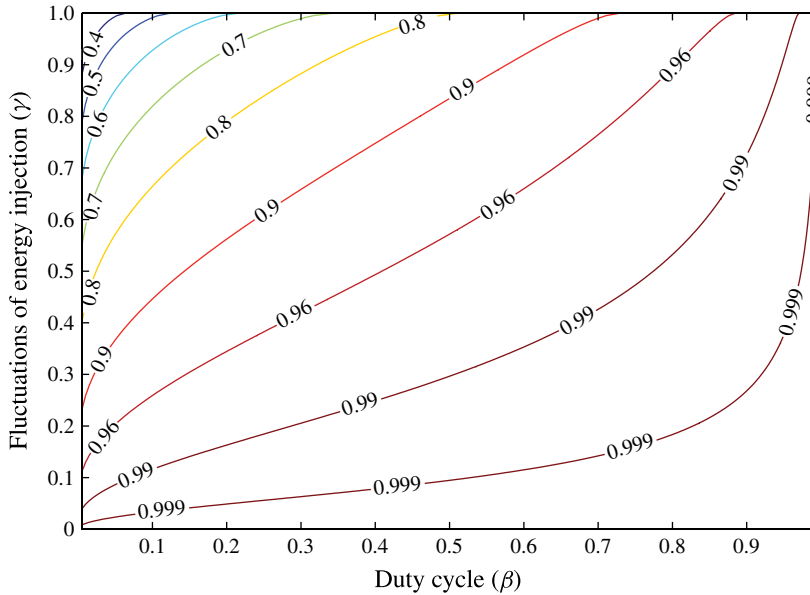
FIGURE 1. (Colour online) Contour plot of the correction factor κ from (1.6) for $p = 2$. This shows the change in the coefficient of the inertial range scaling law as a function of the amplitude of fluctuations in the energy input γ, and the time spent in the high energy input state, or duty cycle, β.

expression

$$\langle (\Delta_r u)^p \rangle = C'_p \frac{\langle \varepsilon^{p/3} L^{\xi_p} \rangle}{\langle \varepsilon \rangle^{p/3} \langle L \rangle^{\xi_p}} (\langle \varepsilon \rangle r)^{p/3} \left(\frac{\langle L \rangle}{r} \right)^{\xi_p}. \tag{1.9}$$

It is important to determine the size of the effects of fluctuations in the large-scale energy input in real turbulent flows. Surprisingly, there are no published results that we know of that document a dependence of coefficients of inertial range scaling laws for structure functions on systematic changes in the large scales of the flow. A compilation of experimental (Sreenivasan 1995) and simulation (Donzis & Yeung 2010) results have given credence to the notion that the second-order coefficients are close enough to independent of the flow that they can be treated as universal constants. At least three experimental studies have explored fluctuations in the large-scale energy input in detail. Praskovsky *et al.* (1993) study two high Reynolds number flows, a mixing layer and a return channel. They find a conditional dependence of the second-order structure functions on the instantaneous velocity and connect this with spatial and temporal variability of the energy flux passing through the cascade. They emphasize that the conditional dependence they observe is not in violation of the assumptions of the refined Kolmogorov theory since changes in the energy flux should change the small scales. Sreenivasan & Stolovitzky (1996) use measurements in the atmospheric boundary layer to demonstrate the conditional dependence of structure functions on the velocity. They identify this conditional dependence as a result of mixed averages over regions of the flow with different energy dissipation rates, and show that when properly normalized by the instantaneous local energy dissipation rate the conditional dependence is removed, in agreement with Kolmogorov's refined similarity hypotheses.

More recently, Mouri *et al.* (2006) explored the effects of large-scale fluctuations of the turbulence energy dissipation rate. They measure grid and boundary layer turbulence and clearly confirm that the large-scale energy fluctuations exist and that they affect small-scale statistics. They explicitly state that the large-scale fluctuations do not affect the power law scaling or the coefficients of second-order structure functions in the inertial range.

There is another set of literature exploring time-dependent energy input in turbulence that has identified the presence of response maxima when the energy input oscillates about a mean value with a period of the order of the large-eddy turnover time. This effect was first predicted in a mean field theory (von der Heydt, Grossmann & Lohse 2003). It has been explored in a variety of models, numerical simulations and experiments (Cadot, Titon & Bonn 2003; von der Heydt *et al.* 2003; Kuczaj, Geurts & Lohse 2006; Bos, Clark & Rubinstein 2007*a*; Jin & Xia 2008; Kuczaj *et al.* 2008). However, this work seems not to have considered the effects on structure functions.

In this paper we present a series of experimental measurements of the effects of time-dependent energy input on the small scales of turbulence. We focus on second-order structure functions where the effects of internal intermittency are small. We find that the coefficient of the inertial range scaling law depends on the fluctuations in the large-scale energy input and measure coefficients that are more than 20 % below the value for the continuously driven case.

2. Experiment

The turbulence is generated in an octagonal Plexiglas tank that is 1 m × 1 m × 1.5 m filled with approximately 1100 l of filtered and degassed water. Two identical octagonal grids oscillate in phase to generate the turbulence. The grids have 8 cm mesh size, 36 % solidity, and are evenly spaced from the top and bottom of the tank with a 56.2 cm spacing between grids and a 1 cm gap between the grids and the tank walls. The grid oscillation has 12 cm amplitude and is powered by an 11 kW motor. In these experiments the grids were oscillated with frequencies up to 4 Hz, which allows Taylor Reynolds numbers up to $R_\lambda = 262$. Details about the experimental setup are available in Blum *et al.* (2010).

We use stereoscopic particle tracking using four cameras as shown in figure 2. The cameras are two Bassler A504K video cameras capable of 1280×1024 pixel resolution at 480 frames per second, and two Mikrotron MC1362 cameras with the same pixel resolution and data rates, but with greater sensitivity. A 5 cm × 5 cm × 5 cm detection volume at the centre of the flow was illuminated with a pulsed 50 W Nd:YAG laser. A real-time image compression circuit with compression factors of 100 to 1000 enables us to acquire data continuously, which allows access to large data sets of particle trajectories (Chan, Stich & Voth 2007).

Previous work with this experiment has shown that there are measurable fluctuations in the energy input even when the driving frequency of the oscillating grids is constant (Blum *et al.* 2010). Here we augment this effect by modulating the driving frequency of the oscillating grids. For example, rather than driving the grids continuously at 3 Hz, we can drive it at 3 Hz for 15 s, and then halt for 15 s, and repeat. This produces a periodic time dependence in the energy input with a longer time scale than the grid oscillation period. Figure 3 shows a schematic of the frequency modulation along with variable definitions. In this paper, we explore three different ways to augment the fluctuations in large-scale energy input: (i) change T, the time to complete one modulation cycle; (ii) change the frequency modulation by holding f_{high}
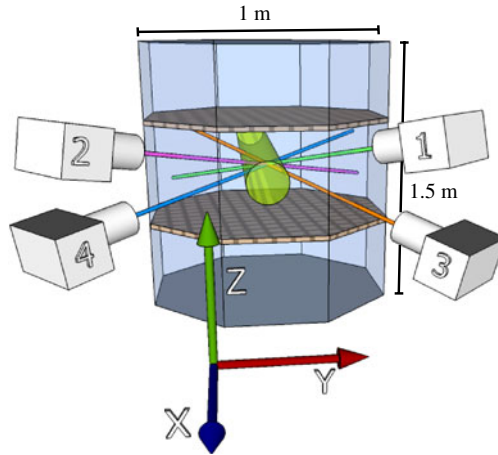
FIGURE 2. (Colour online) Experimental setup. Four high-speed cameras obtain stereoscopic images of a $(5 \text{ cm})^3$ volume at the centre of the flow that is illuminated by a pulsed Nd:YAG laser with 50 W average power.
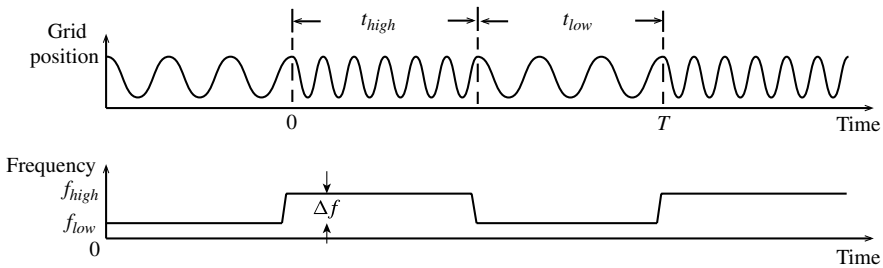

FIGURE 3. Sketches of the position and frequency of the oscillating grids as functions of time. t_{high} is the time over which the grids oscillate at the higher frequency, t_{low} is the time at lower frequency. T is the cycle period, the time to complete one cycle of modulation from high to low frequency. f_{high} is the high frequency of grids and f_{low} is the low frequency. Δf is the frequency differences between f_{high} and f_{low}.

constant and changing f_{low} from 0 up to f_{high}; and (iii) changing the duty cycle t_{high}/T. Figure 4 shows a specific example of the time dependence of the mean square velocity, $\langle u_i u_i \rangle$, which is a measure of the energy in the large scales. The mean is obtained as a phase average over many cycles. It takes time for energy to propagate from the grid to the detection volume, so the energy lags several seconds after the grid frequency changes.

    The inertia of the system used to drive the grids limited the rate at which the driving frequency could be changed. We were able to reduce the time required to stop or start to less than 1/3 of a second by minimizing the inertia in the experiment. The original version of this apparatus (Blum *et al.* 2010) used a flywheel to improve symmetry between the up and down stroke of the oscillating grids. For this experiment we replaced the flywheel with a coupler. For the run with $f_{high} = 3$ Hz shown in figure 4, the start time is less than one oscillation and accounts for less than 3 % of the data. However, limitations from the inertia of the drive system did limit our experiments to
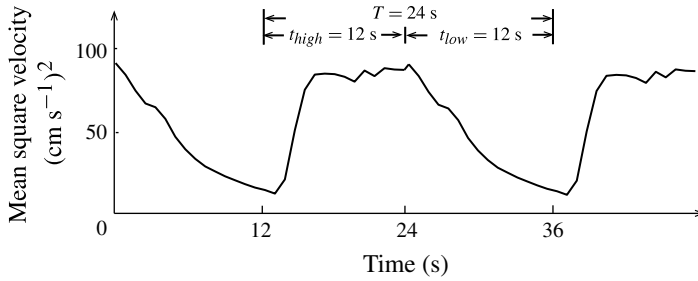
FIGURE 4. Time dependence of the mean square velocity measured by phase averaging over many cycles for an experiment with $f_{high} = 3$ Hz, $f_{low} = 0$ Hz, period $T = 24$ s, and 50 % duty cycle. Both the first and second cycle are phase averages over the whole experiment and hence are identical.

	f_{high} (Hz)	f_{low} (Hz)	T (s)	Duty cycle (%)	U (cm s^{-1})	L (cm)	τ (s)	ε (cm^2 s^{-3})	R_λ
	3	3	30	50	5.46	7.11	1.3	22.9	241
Varying	3	2	30	50	4.72	7.06	1.5	14.9	224
amplitude	3	1	30	50	4.23	6.47	1.57	11.7	203
	3	0	30	50	4.21	6.72	1.59	11.1	206
	3	0	3	50	4.44	7.55	1.72	11.6	224
	3	0	6	50	4.71	8.04	1.71	13	238
Varying	3	0	12	50	4.54	7.86	1.72	11.9	231
period	3	0	24	50	4.42	7.57	1.73	11.4	224
	3	0	48	50	4.07	6.07	1.49	11.1	193
	3	0	384	50	4.06	5.82	1.36	11.5	188
	3	0	30	100	5.46	7.11	1.3	22.9	241
Varying	3	0	30	75	4.92	7.22	1.47	16.5	230
duty cycle	3	0	30	50	4.21	6.72	1.6	11.1	206
	3	0	30	25	3.27	6.24	1.91	5.6	175
Varying	1	N/A	N/A	100	1.96	6.38	3.28	1.18	137
Reynolds	2	N/A	N/A	100	4.05	8.8	2.17	7.55	231
number	3	N/A	N/A	100	5.46	7.11	1.3	22.9	241
	4	N/A	N/A	100	7.14	6.42	0.73	56.7	262

TABLE 1. Experimental parameters and resulting statistics for different sets of experiments. The length scale characterizing the energy input is $L = u^3/\varepsilon$. The eddy turnover time is $\tau = L/U$. Note that the case of $f_{high} = 3$ Hz, $f_{low} = 3$ Hz, duty cycle 50 % corresponds to the same data as the case of $f_{high} = 3$ Hz, $f_{low} = 0$ Hz, duty cycle 100 %.

periods of $T = 3$ s and greater, which resulted in the period of the modulation of the energy input always being longer than the large-scale turnover time.

We conducted three sets of experiments to explore the effects of fluctuations of large-scale energy input on small scales. Parameters for each of the experiments are given in table 1. In the first set of experiments we made measurements with period T of 3, 6, 12, 24, 48, and 384 s while always modulating the grid frequency with $(f_{high}-f_{low}) = (3-0)$ Hz, with a duty cycle of 50 %. We will refer to these experiments as 'varying the period'. In the second set of experiments, we

held $f_{high} = 3$ Hz and made measurements with f_{low} of 3, 2, 1, and 0 Hz to get $(f_{high}–f_{low}) = (3–3), (3–2), (3–1), (3–0)$ Hz with $T = 30$ s period and 50 % duty cycle. We will refer to these experiments as 'varying the amplitude'. In the third set of experiments we made measurements with duty cycles of 25, 50, 75 and 100 %, while always modulating the grid frequency with $(f_{high}–f_{low}) = (3–0)$ Hz and a period of $T = 30$ s. We will refer to these experiments as 'varying the duty cycle'. We also took data with continuous drive at grid frequencies ranging from 1 to 4 Hz to vary the Reynolds number as our control group, to show that the effects we observe cannot be simply attributed to the changes in Reynolds number.

In figure 5(*a*) we show the time dependence of the mean square velocity, $\langle u_i u_i \rangle$, for the set of experiments varying the period. Time zero is defined as the time when the energy input halts. For all of these experiments, the energy dissipates at approximately the same rate, so the decay curves nearly collapse. After half a period, the energy input resumes. For the experiments of longer period such as $T = 48$ s, the energy has decayed to 10 % of its initial value after half a period. In figure 5(*b*), these data are shown with time normalized by the period. One additional data set with $T = 384$ s is added in this plot. Only for this data set with a very long period does the fluid become approximately quiescent before the energy input is resumed.

3. Results

3.1. *Coefficients of the inertial range scaling law*

3.1.1. *Varying period*

Figure 6 shows the third-order structure functions of the experiments varying the period. When compensated by εr, the inertial and dissipation ranges of the third-order structure functions collapse fairly well.

The energy dissipation rate is determined from the peak value of these compensated third-order structure functions and the 4/5 law. It is known that this method will slightly underestimate the energy dissipation rate for the moderate Reynolds numbers that we study. From previous simulations (Ishihara, Gotoh & Kaneda 2009) and experiments (Moisy, Tabeling & Willaime 1999), we estimate that this error is between 5 and 10 %. This is consistent with an estimate from our own data in which adding the viscous term in the Kolmogorov equation produces a value of the energy dissipation rate between 7 and 10 % higher than the value from the 4/5 law. We choose to use the 4/5 law estimate of the energy dissipation rate because we will focus on measurements of the second-order Kolmogorov constant. The small underestimate of that quantity due to moderate Reynolds number is partially cancelled by the underestimate of the energy dissipation rate, leading to measurements of the Kolmogorov constant that are closer to the high Reynolds number value.

However, the compensated second-order structure functions shown in figure 7(*a*) do not collapse well at all. The maximum of these compensated structure functions, which is an estimate of the coefficient in the inertial range scaling law, shows a 20 % decrease as the period increases. Increasing the fluctuations in the energy input does have a significant effect on the small scales of the flow. The shape of the second-order structure functions shows little change, which is consistent with the idea that fluctuations in the energy input at large scales primarily change the coefficients in scaling laws while leaving the scaling exponents unchanged. Figure 7(*b*) shows the second-order structure functions scaled by the prediction of (1.8). The good collapse of these curves after scaling indicates that the effects of fluctuations in the energy input are largely captured by the refined model.
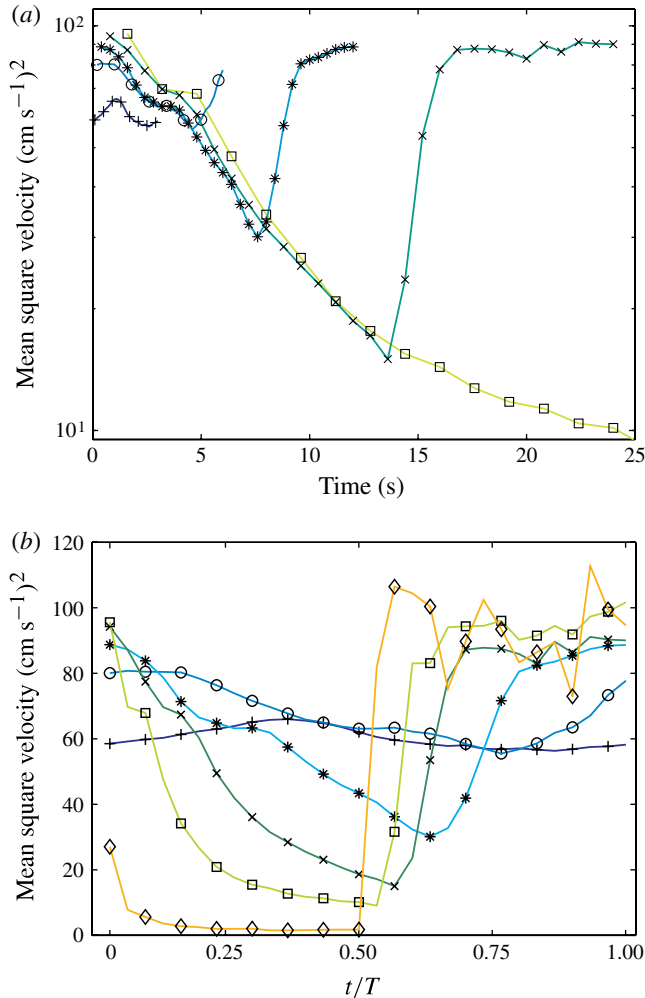
FIGURE 5. (Colour online) (*a*) Time dependence of the mean square velocity measured by phase averaging over many cycles. The motor is halted at $t = 0$, and turned back on after half a cycle period, $t = T/2$. Data are from the experiments with varying cycle period: $T = 3$ s ($+$), 6 s ($\bigcirc$), 12 s ($*$), 24 s ($\times$), 48 s ($\square$). The symbols $\bigcirc$ and $+$ are only plotted every four data points for clarity, and other symbols show every data point. (*b*) The fluctuating energy versus t/T with an additional data set $T = 384$ s ($\diamond$). Here all data sets have symbols plotted for every other data point.

Figure 8 shows the measured coefficient of the inertial range scaling of the second-order structure function, commonly labelled as Kolmogorov constant C_2. We use the peak of the compensated structure functions in figure 7(*a*) to measure C_2. The decrease in the 'constant' C_2 as the period increases is a clear indication that the previous assessment by Praskovsky *et al.* (1993) and Mouri *et al.* (2006) that large-scale fluctuations do not affect second-order structure functions is only an approximation that is valid in cases where the fluctuations in the energy input are small. Figure 8 also shows the prediction of our refined model from (1.8) with the model value of $C_2 = 2.0$. The experimental measurement and the refined model
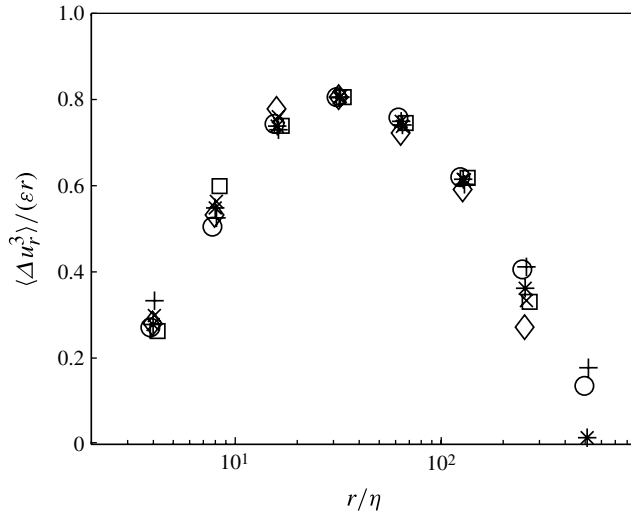
FIGURE 6. Third-order compensated structure functions for the experiments with varying cycle period: $T = 3$ s (+), 6 s (○), 12 s (∗), 24 s (×), 48 s (□), 384 s (◇). The driving frequency modulation is $(f_{high}$–$f_{low}) = (3$–$0)$ Hz and the duty cycle is 50 %.

are in fairly good agreement. There are many possible factors that contribute to the difference between the measurements and the model, including the difficulty in measuring scaling coefficients at modest Reynolds number and limitations of the estimate $\varepsilon \propto U^3/L$ in (1.7). These flows with $f_{low} = 0$ contain both forced and decaying turbulence, which has been observed to have different corrections for finite Reynolds numbers (Antonia & Burattini 2006) and different coefficients in the relation $\varepsilon \propto U^3/L$ (Bos, Shao & Bertoglio 2007b). The dashed line is the prediction of the model by Monin and Yaglom. Our experimental value of C_2 approaches this dashed line when the period is long, as it should, since in that case we are approaching the situation Monin and Yaglom consider where the energy input is constant in time for both the low-frequency and high-frequency states.

Measurement of inertial range scaling coefficients from these data at modest Reynolds numbers presents some difficulties. We have tried different methods to determine the coefficients. Averaging the three bins at the maxima of both the third- and second-order structure functions produces energy dissipation rates that are smaller by up to 9 % while yielding changes of up to 5 % in the measured values of C_2. These differences have no effect on the conclusions we draw. Data at larger Reynolds numbers will be necessary to provide more precise quantitative measurements of how scaling coefficients depend on fluctuations in the energy input, but our data clearly show a dependence that is several times larger than our measurement uncertainty.

3.1.2. *Varying amplitude*

Similar effects of large-scale energy fluctuations on small scales are also seen in the experiments where the amplitude of the energy input is varied by changing the grid oscillation frequency. Figure 9(a) shows the second-order compensated structure functions for the data sets with varying amplitude. Similar to the experiments varying the period, the curves do not collapse, indicating that the coefficient of the scaling law depends on the large scales. Figure 9(b) shows the second-order structure functions scaled by the prediction of (1.8). The better collapse of these curves after scaling
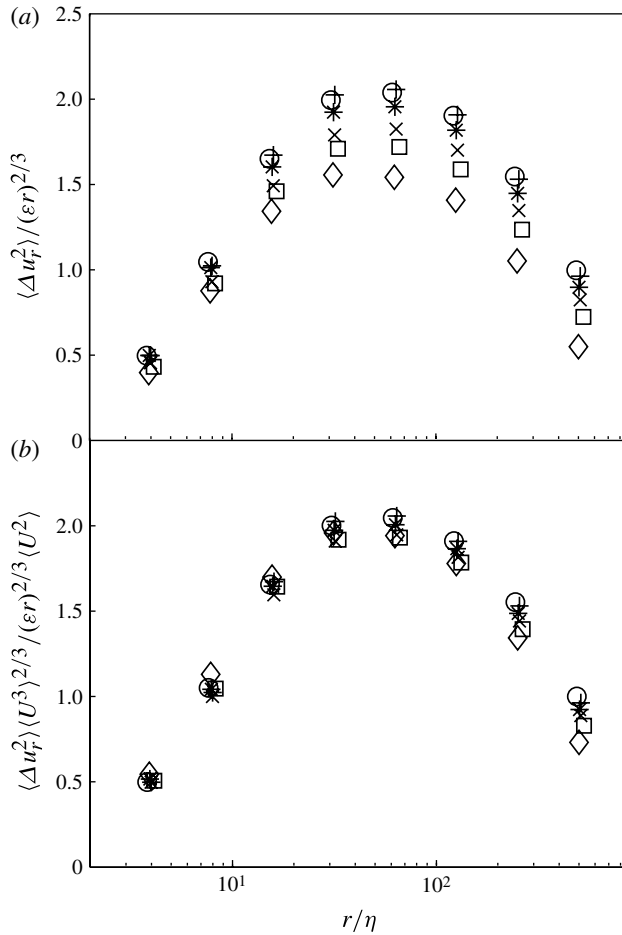
FIGURE 7. (*a*) Second-order compensated structure functions for the experiments with varying period. Symbols are the same as in figure 6. (*b*) Second-order structure functions scaled by the ratio of moments of the energy dissipation rate predicted by the refined model in (1.8).

again indicates that the refined model is accurately describing the effects of fluctuating energy input.

Figure 10 shows the measured Kolmogorov constants C_2 along with predictions from the refined model and the Monin and Yaglom model. The main point is that increasing the amplitude of the fluctuations in the energy input systematically decreases the constant as predicted. Quantitatively, the refined model has coefficients larger than those measured, meaning that it underestimates the effect of the large-scale fluctuations. This deviation is probably due to the refined model using the time dependence of the root mean square velocity to estimate the fluctuations in the energy input, but this does not capture all of the fluctuations. The Monin and Yaglom model works well for small amplitudes of the energy input fluctuations, but for the largest fluctuation amplitude $(3 - 0)$ Hz, it predicts a much larger effect of the large-scale fluctuations than are observed experimentally. This is expected since these data are for period $T = 30$ s, and at large amplitudes of the energy input fluctuations, there is not
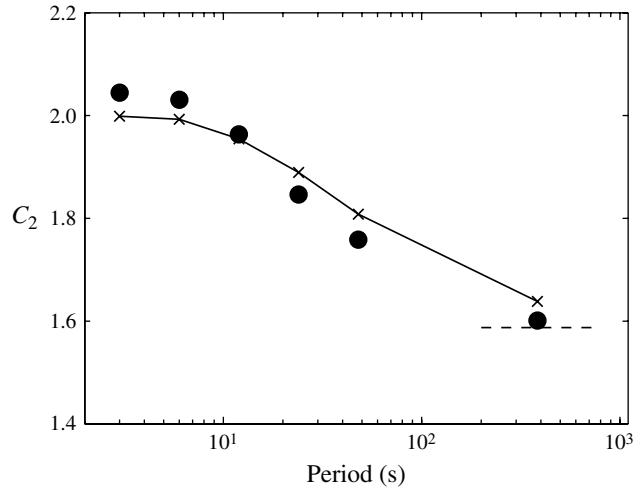
FIGURE 8. Experimental measurements of Kolmogorov constant C_2 (●) along with the prediction of the refined model (×) for the experiments of varying period. The dashed line represents the prediction of the model by Monin and Yaglom.

enough time for the energy to decay to the constant values assumed by the Monin and Yaglom model.

For the experiments varying the amplitude of the fluctuations in the energy input, we did not directly measure the phase-averaged fluctuating velocity needed in the refined model. To make predictions with this model, we had to model the fluctuation velocity using the known values for continuous driving at different frequencies and the decay rate data in figure 5. The limitations of this model probably also contribute to the poorer agreement with the refined model in this case.

3.1.3. *Varying duty cycle*

The set of experiments varying the duty cycle in figure 11 also shows that the compensated second-order structure functions show strong dependence on fluctuations in the energy input. We show the measured Kolmogorov constant C_2 in figure 12. When the duty cycle is smaller, we observe a smaller Kolmogorov constant. For the 25 % duty cycle we see the smallest value of the Kolmogorov constants of any data set with $C_2 = 1.62$. Note that the 25 % duty cycle and the 75 % duty cycle do not have the same C_2. Because times with large energy input dominate the moments of the energy dissipation rate, the effects on the Kolmogorov constant are largest for low duty cycles, where bursts of large energy input are followed by a long quiescent period.

The predictions of the Monin and Yaglom model shown in figure 12 are consistently below the measured constants. We expect that if the experiments were performed for a larger period rather than $T = 30$ s, they would approach the Monin and Yaglom predictions.

3.1.4. *Varying Reynolds number*

The set of experiments varying the Reynolds number for constant energy input in figure 13 shows that the Kolmogorov constants for the second-order structure functions do not have a strong dependence on Reynolds number. We vary the Reynolds number from $R_\lambda = 137$ at 1 Hz continuous driving to $R_\lambda = 262$ at 4 Hz continuous driving. The shape of the structure function changes at the lowest Reynolds number as
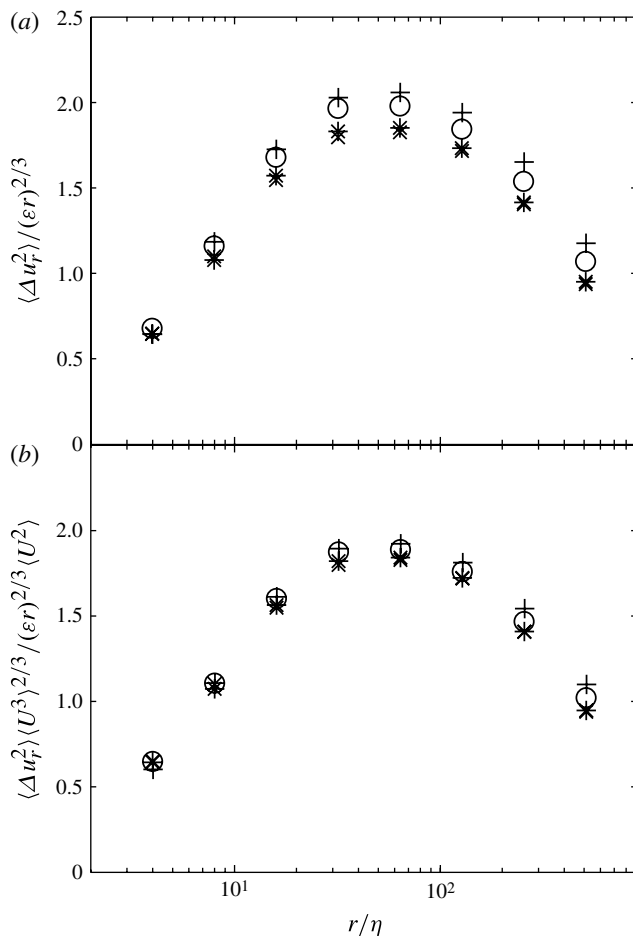
FIGURE 9. (*a*) Second-order compensated structure functions for the experiments with varying amplitude. (*b*) Second-order structure functions scaled by the ratio of moments of the energy dissipation rate predicted by the refined model. Symbols represent different frequency modulations: $(f_{high}-f_{low})$ = (3–3) Hz (+), (3–2) Hz (○), (3–1) Hz (∗), (3–0) Hz (×). The cycle period T is 30 s, and the duty cycle is 50 %.

expected, but after using the third-order structure functions to determine the energy dissipation rate, the peak value remains relatively constant. There is a slight trend for the peak to become larger for lower Reynolds numbers. This trend is in the opposite direction to the variations we observe due to fluctuations in the energy input, and significantly smaller. Our measurements in flows with large fluctuations in the energy input rate have slightly smaller Reynolds numbers and significantly smaller values of the Kolmogorov constants than the steadily driven flows. This indicates that the variation we observe in the Kolmogorov constant is not simply the result of different effective Reynolds numbers in different experiments.

3.2. *Conditional structure functions*

Previous work has used conditional structure functions to quantify the effects of the large scales on small scales in turbulent flows (Praskovsky *et al.* 1993; Sreenivasan &
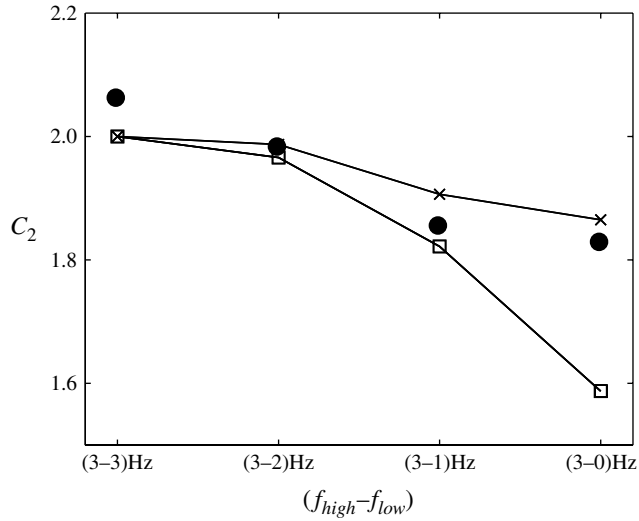
FIGURE 10. Experimental measurements of Kolmogorov constant C_2 (●), compared with predictions from the refined model (×), and the Monin and Yaglom model (□) for the experiments of varying amplitude. The predictions of the refined model and the Monin and Yaglom model assume $C_2 = 2$.
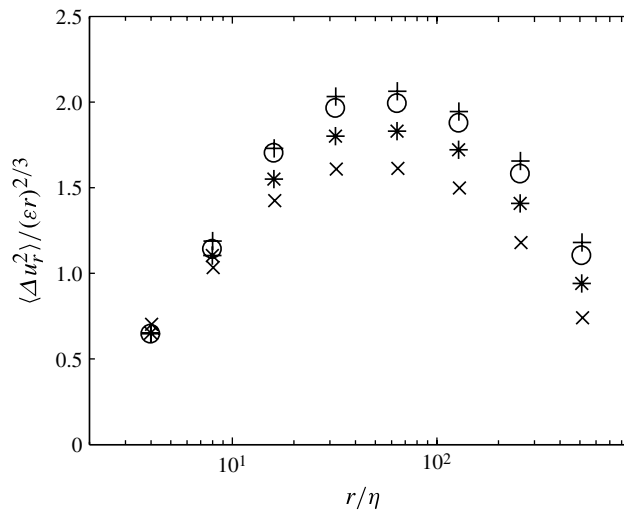

FIGURE 11. Second-order compensated structure functions for the experiments with varying duty cycle: 100 % (+), 75 % (○), 50 % (∗), 25 % (×). The driving frequency modulations are $(f_{high} - f_{low}) = (3–0)$ Hz and the period T is 30 s.

Stolovitzky 1996; Sreenivasan & Dhruva 1998; Blum *et al.* 2010, 2011). Velocity differences between two points separated by *r* are dominated by structures near *r* in scale, while velocity sums of two points are dominated by the large scales in the flow. So moments of velocity differences conditioned on sums provide a convenient way to observe the effects of the largest scales on other scales. We
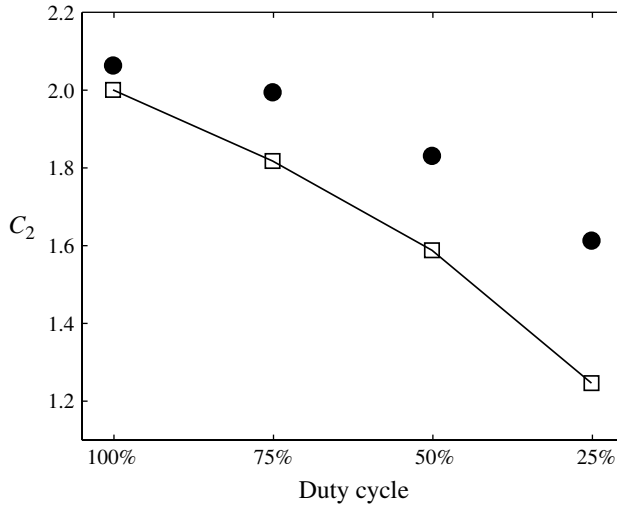
FIGURE 12. Experimental measurements of Kolmogorov constant C_2 ($\bullet$), and the prediction of Monin and Yaglom model ($\square$) for the experiments of varying duty cycle.
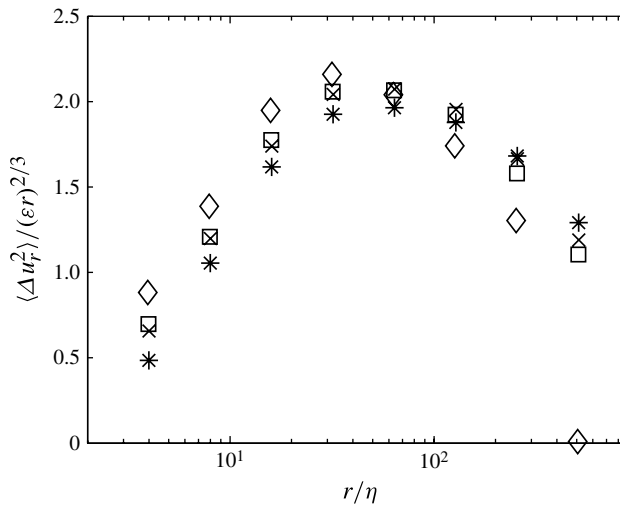

FIGURE 13. Second-order compensated structure functions for the experiments with varying Reynolds numbers: $R_\lambda = 262$ ($*$), 241 ($\times$), 231 ($\square$), 137 ($\diamond$).

find that conditional structure functions provide a more sensitive measurement of the existence of fluctuations in the large-scale energy input than the coefficients of inertial range structure functions. However, theoretical tools to predict the effects of large-scale fluctuations on conditional structure functions are not available. In this section we present measured conditional structure functions as we systematically change the fluctuations in the energy input.

3.2.1. *Varying amplitude*

Figure 14 shows conditional structure functions for the data sets varying the amplitude of the fluctuations in the energy input. We condition the structure function on the velocity component that is transverse to r and denoted by $\Sigma u_\perp$. In order to
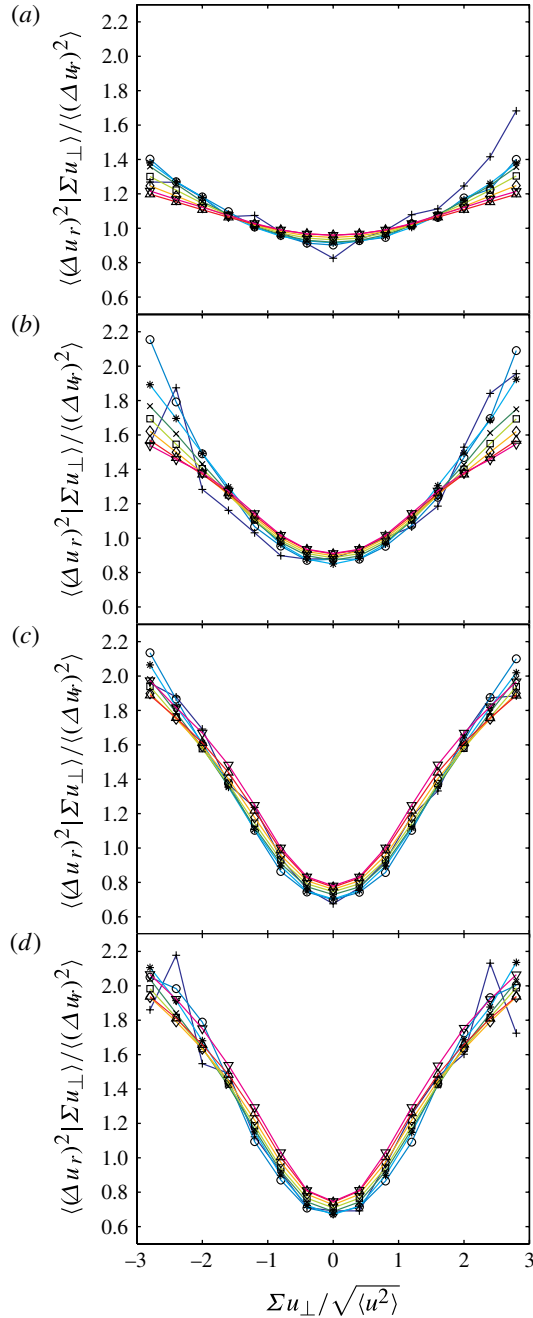
FIGURE 14. (Colour online) Eulerian second-order conditional structure function versus large-scale velocity for the experiments with varying amplitude. The frequencies modulated were $(f_{high}-f_{low}) = (3–3)$ Hz (*a*), (3–2) Hz (*b*), (3–1) Hz (*c*), (3–0) Hz (*d*). The curves represent the separation distances: $r/\eta = 2.67$–5.33 (+), 5.33–10.67 (○), 10.67–21.33 (∗), 21.33–42.67 (×), 42.67–85.33 (□), 85.33–170.67 (◇), 170.67–341.33 (△), 341.33–682.67 (▽).

compare the conditional structure function for different length scales, we normalize the vertical axis by the unconditioned structure function. The horizontal axis is normalized by the characteristic velocity $U = (\langle u_i u_i /3\rangle)^{1/2}$. In figure 14(*a*) for constant driving of the oscillating grids, we see the results published by Blum *et al.* (2010) that the conditional structure functions for all length scales show a similar dependence on the large-scale velocity. There is a slight dependence on length scale, with the smallest length scales showing a stronger dependence on the large-scale velocity. This small dependence on length scale remains unexplained since it is the opposite of the expectation that the small scales are approaching universality. The same effect is seen in direct numerical simulation data in Blum *et al.* (2011). However, in this paper we focus on fluctuations of the energy input, and we will see that these produce much bigger effects than the small differences for different length scales.

Figures 14(*b*)–14(*d*) show that increasing the fluctuations in the energy input produces a large increase in the dependence of the conditional structure functions on the large-scale velocity. In each subfigure the curves for different length scales remain very similar, which confirms the fact observed earlier that fluctuating energy input does not change the length scale dependence. It primarily changes a prefactor scaling the entire structure function. Note that figure 14(*a*) still has dependence on the large-scale velocity even though the oscillating grid is driven at a constant 3 Hz frequency. We interpret this as fluctuations in the energy input that remain even in the case of constant driving (Blum *et al.* 2010). To more directly compare the effects of changing the energy input fluctuations, we extract the curve for $r/\eta = 10.7$–21.3 from figure 14(*a*–*d*) and plot them on one graph as shown in figure 15(*a*). In figures 14 and 15 the symmetry around zero large-scale velocity is a result of conditioning on the transverse component of the large-scale velocity, for which $\Sigma u_\perp > 0$ is indistinguishable from $\Sigma u_\perp < 0$.

To quantify the observed dependence of the conditional structure function, we fit all the curves in figure 14 to the functional form $au^4 + bu^2 + c$. Figure 15(*b*) shows the fit coefficient *b* as a function of the separation distance r/η. The coefficient *b* measures the curvature of the conditional structure functions at the origin, and it captures the primary dependence on the large-scale velocity. Measuring the coefficient of the second-order term *b* is also in keeping with a previous study (Sreenivasan & Dhruva 1998). There is an increase by more than a factor of 5 in the curvature, *b*, as the fluctuations in the energy input increase from driving at 3 Hz continuously to alternating between 3 and 0 Hz. The degree to which all length scales show similar dependence on the large scales can also be evaluated from figure 15(*b*). In §3.3 we will show that changes in *b* are closely related to the changes in the Kolmogorov constant that we presented in §3.1.

3.2.2. *Varying period*

Figure 16(*a*) shows the conditional second-order structure functions for the experiments with varying period. When period *T* increases, there is a stronger dependence on large-scale velocity. The two shortest periods $T = 3$ s and 6 s have similar and relatively low curvatures. Increasing the period allows the turbulence to decay closer to quiescent before the energy input resumes, so the conditional dependence on the large-scale velocity is stronger at longer periods. For the very long period, $T = 384$ s, the conditional structure function has a different shape with a sharp minimum at the centre of a region with less curvature. This is the result of the high energy state providing the samples with large velocity sum, while the low energy state
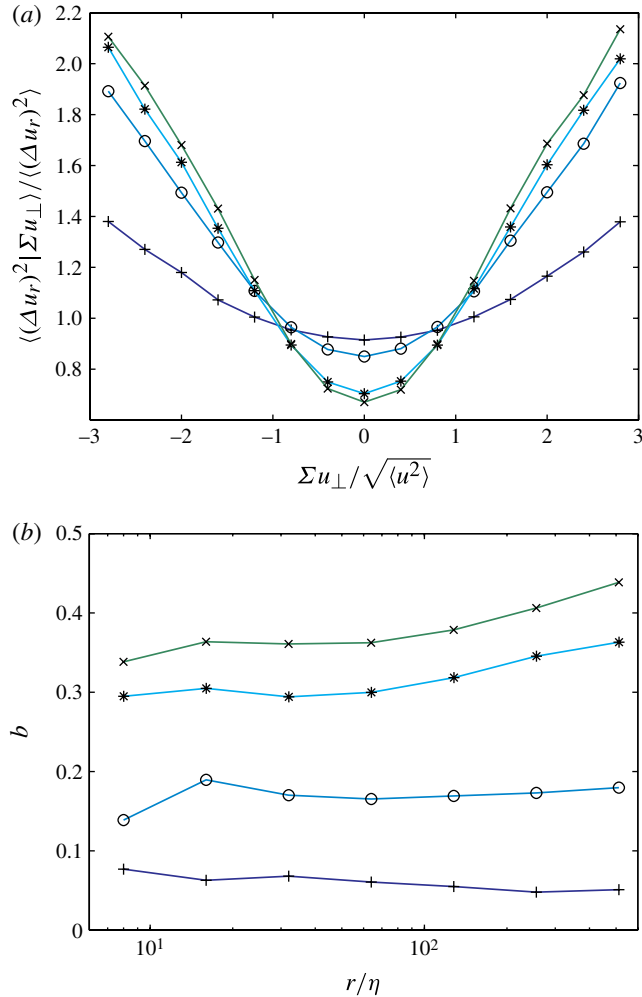
FIGURE 15. (Colour online) (*a*) The velocity dependence of conditional second-order structure functions of one separation distance $r/\eta = 10.67$–21.33 for the experiments with varying amplitude: $(f_{high}$–$f_{low}) = $ (3–3) Hz (+), (3–2) Hz (○), (3–1) Hz (∗), (3–0) Hz (×) with 50 % duty cycle and $T = 30$ s. (*b*) The coefficient b as a function of the separation distance for the experiments with varying amplitude. Symbols are the same as in (*a*).

provides only samples with velocity sum near zero. For these data at $T = 384$ s there is also a much stronger dependence on the length scale, as shown in figure 16(*b*).

3.2.3. *Varying duty cycle*

Figure 17(*a*) shows the second-order conditional structure functions for the experiments with varying duty cycle. It shows that reducing the duty cycle produces a large increase in the dependence of the conditional structure functions on the large-scale velocity. The result is consistent with our previous findings that increasing the fluctuations of the large-scale energy input increases the dependence of the second-order conditional structure functions on the large-scale velocity. Here all length scales show fairly similar dependence on the large scales, as seen in figure 17(*b*).
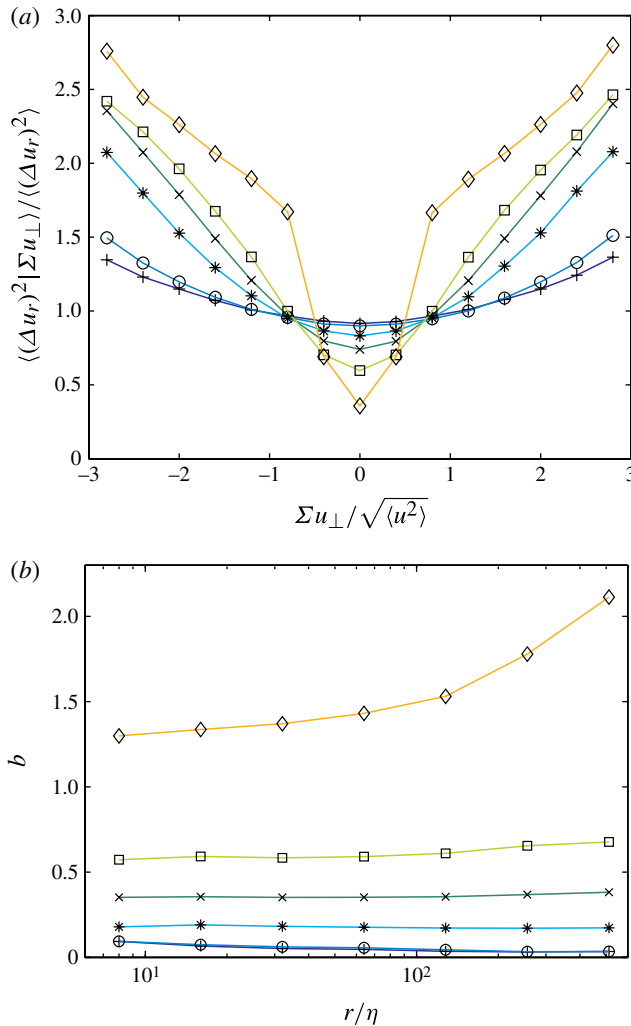
FIGURE 16. (Colour online) (*a*) The velocity dependence of second-order conditional structure functions of one separation distance $r/\eta = 10.67–21.33$ for the experiments with varying cycle period: $T = 3$ s (+), 6 s (○), 12 s (∗), 24 s (×), 48 s (□), 384 s (◇). The driving frequency modulations are $(f_{high}–f_{low}) = (3–0)$ Hz, and the duty cycle is 50 %. (*b*) The coefficient *b* as a function of separation distance for the experiments with varying period. Symbols are the same as in (*a*).

3.3. *Connecting conditional structure functions and coefficients of inertial range scaling laws*

The curvature *b* of the conditional structure functions increases as the fluctuations of the large-scale energy input increase. This suggests that it might be possible to connect *b* with changes in the coefficients of inertial range scaling law presented in § 3.1.

A simple linear parametrization $C_2 = 2(1 − 0.15b)$ seems to match the measured scaling coefficients fairly well, as shown in figure 18. However, we do not have a solid theoretical foundation for choosing this functional form and the value of 0.15 is
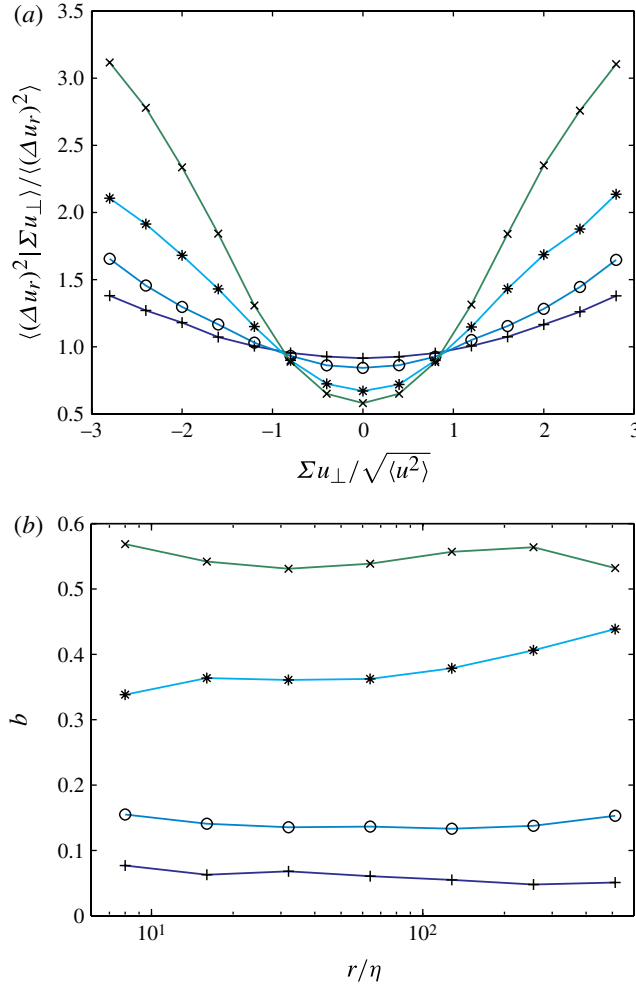
FIGURE 17. (Colour online) The velocity dependence of conditional second-order structure functions of one separation distance $r/\eta = 10.67$–21.33 for the experiments with varying duty cycle: 100 % (+), 75 % (○), 50 % (∗), 25 % (×), with driving frequency modulations $(f_{high}$–$f_{low}) = (3$–$0)$ Hz and period $T = 30$ s. (b) The coefficient b as a function of separation distance for the experiments with varying duty cycle. Symbols are the same as in (a).

a rough fit. For weak fluctuations in the energy input, which includes most turbulent flows of interest, this parametrization seems to work fairly well. But for extreme cases it fails. At low duty cycles in figure 18(b), this parametrization is well above the measured coefficient. In the limit where one of the states is actually quiescent ($\gamma = 1$ in figure 1), the curvature b should go to infinity while the coefficient of the scaling law would not go to zero. Conditional structure functions and coefficients of inertial range scaling laws are both modified by fluctuations in the large-scale energy input of turbulence. A more complete understanding of the relationship between these two could be very useful, since the effects of fluctuations in the large-scale energy input are much easier to measure using conditional structure functions.
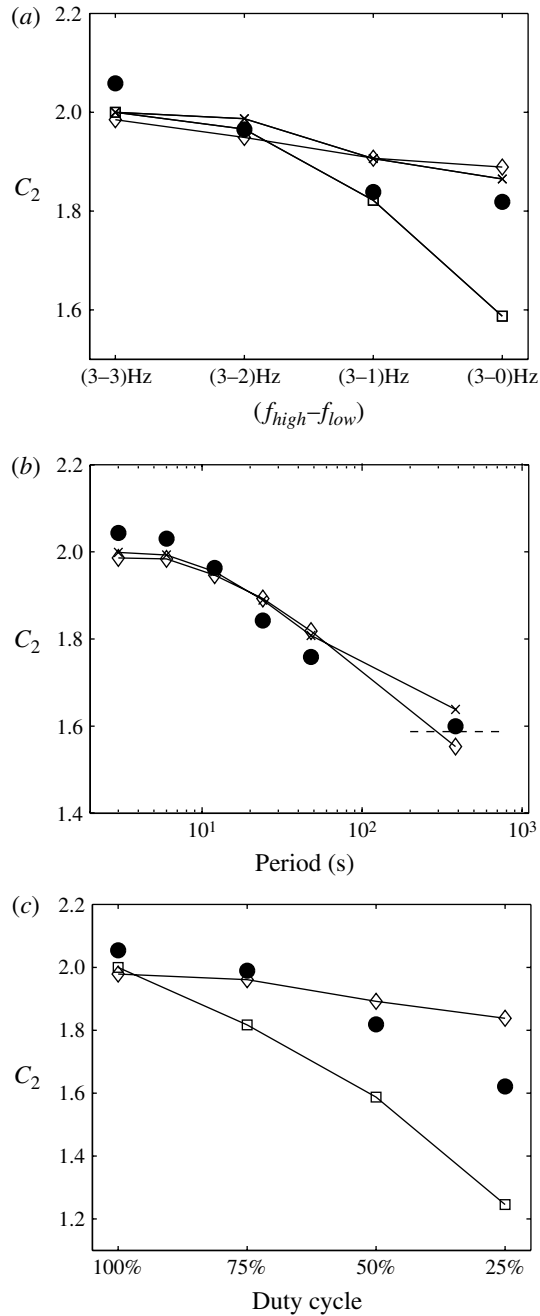
FIGURE 18. The relationship of the curvature b of the conditional second-order structure function with the coefficient of the inertial range scaling law: (*a*) varying the amplitude, (*b*) varying the period, and (*c*) varying the duty cycle. Symbols: $\diamond$, the parametrization $2(1 - 0.15b)$; $\bullet$, the experimental measurements of the Kolmogorov constant C_2; $\times$, the refined model; $\square$, the Monin and Yaglom model.

4. Discussion

In this paper we have focused on inertial range effects of fluctuations in the energy input because they are most easily measured with our apparatus. But it should be noted that the non-universality of the inertial range scaling coefficients implies non-universality of the functional form of structure functions in the dissipation range. Because the Kolmogorov scale depends on the energy flux, the functional form in the dissipation range will depend on the distribution of the energy flux, which depends on the fluctuations of the energy input at large scales.

A problem facing research into the effects of large-scale fluctuations on the small scales of turbulence is that the terminology that has accumulated over many years is not always as clear as it could be. The word 'intermittency' appears to have entered the turbulence literature to describe the fluctuations between turbulent and non-turbulent fluid flowing past a point in a free shear flow. For example, the textbook by Hinze in 1959 uses 'intermittent' only in this sense. The second edition of this textbook (Hinze 1975) introduces the use of a flatness factor to measure the 'degree of intermittency' (p. 242), but even here, the goal is to quantify the fraction of the time that turbulence occurs. Over the decades a major change has occurred in how the word intermittency is used. In the parlance of a large part of the turbulence research community, intermittency has become associated with the rare events of large dissipation that are responsible for anomalous scaling (Sreenivasan & Antonia 1997). A good example of this usage is the book by Frisch (1995) which uses the word 'intermittency' to refer to the fluctuations produced by uneven energy transfer through the cascade, which we refer to above as internal intermittency. Frisch briefly describes the turbulent/non-turbulent fluctuations seen in free shear flows with a footnote that says 'This phenomenon is known as "external intermittency"; its relation to the intermittency discussed in Chapter 8 is not clear.' In general use, the word 'intermittency' has often taken on a connotation about large deviations from the mean that is entirely absent in the standard English definition of the word or in the traditional application of this word to turbulent flows. However, the earlier terminology is also still used. In the textbook by Pope (2000), the word intermittency is reserved for the turbulent/non-turbulent fluctuations in free shear flows, while small-scale effects are called 'internal intermittency'. Other sources use the phrase 'large-scale intermittency' to refer to the turbulent/non-turbulent fluctuations in free shear flows. (Mi & Antonia 2001).

In this paper, we quantify the effects that fluctuations in the energy input at large scales have on the coefficients of inertial range power laws. The success of models based on the refined similarity hypotheses suggests we should use terminology that connects this phenomenon with the closely related phenomenon of internal intermittency that is already widely understood. However, the history of the terminology for these phenomena makes it difficult to find suitable terms. Davidson (2004) provides a clear description of the phenomenon of fluctuations at large scales and uses the phrases 'integral-scale intermittency' and 'large-scale intermittency' to refer to them in his section 6.5.1. We prefer this terminology, but the possibility of confusion with the older use of the phrase 'large-scale intermittency' led us not to use this terminology in this paper.

One way to view the contributions from this and a previous sequence of papers (Blum *et al.* 2010, 2011) is that in quantifying the effects of large-scale fluctuations on small scales, we find that large-scale fluctuations which affect the entire cascade are a standard feature of turbulence and not a special feature of free shear flows or periodically modulated flows. Conditional structure functions are a sensitive way

to quantify this dependence, and with them we find that the effects of large-scale fluctuations can be detected in all flows except for a few special cases such as turbulence behind a passive grid (Blum *et al.* 2011). This observation is in contrast to the usual assessment (see e.g. Praskovsky *et al.* 1993 and Mouri *et al.* 2006), where the large-scale fluctuations are viewed as not affecting second-order statistics except in free shear flows where conditional sampling of the turbulent regime can be used to restore the universal result.

Our interpretation is that, in general, turbulent flows have fluctuations in the large-scale energy input. In many cases these are not large enough to have measurable effects on second-order statistics, but by explicit control of the time dependence of the energy input we can make these effects big enough to produce a 20 % change in the Kolmogorov constant for the second-order structure function. In other flows that appear to have constant energy input such as boundary layers, or von Kármán flow between counter-rotating disks, the strong inhomogeneity allows fluctuations at the large scales to intermittently transport fluid from different parts of the flow, creating fluctuations in the energy input rate which should change the constants in inertial range scaling law in ways predicted by (1.2). The effects of turbulent/non-turbulent fluctuations in free shear flows are then seen to be a special case of this more general problem of transport in an inhomogeneous flow by the large-scale fluctuations. To be sure, it is an extreme case, where the entrained fluid has no vorticity and the viscous super-layer separating turbulent from non-turbulent fluid can be very thin. But the extreme case is smoothly connected to other flows where the large-scale fluctuations entrain fluid with different turbulence characteristics. For example, experiments in a shearless mixing layer (Veeravalli & Warhaft 1989; Kang & Meneveau 2008) can continuously vary the turbulence on the two sides of the mixing layer from the extreme case of turbulent to non-turbulent to the case where the turbulence on both sides of the layer are the same.

In the future, we hope that the community can adopt some terminology that will allow us to talk more clearly about fluctuations at the large scales of turbulence. We have shown here that we can quantify and predict the the effects of large-scale fluctuations using a refined similarity framework. These large-scale fluctuations destroy universality in the Kolmogorov (1941) sense in exactly the way that Landau predicted, and they seem to naturally be called 'large-scale intermittency' since they are to the large scales what internal intermittency is to inertial and dissipation range scales. Furthermore, they are the general case into which the traditional use of the phrase 'large-scale intermittency' can cleanly fall. We hope that further work on this topic will develop tools to more precisely quantify the fluctuations at large scales, and that this will lead to a consensus about the terminology to use in discussing these effects.

5. Conclusion

Previous research has established that the small scales in turbulence are not entirely independent of the large scales (Kolmogorov 1962; Mouri *et al.* 2006; Blum *et al.* 2010). Landau's footnote remark suggests that the fluctuations in the energy dissipation due to non-universal large scales will destroy the universality of small scales. Kolmogorov's paper on the refined similarity hypotheses (Kolmogorov 1962) identified the fact that the coefficients of scaling laws will not be universal. However, during the extensive effort to understand internal intermittency, the effects of fluctuations in the large scales have been largely ignored. The consensus in the literature has been that the coefficient of the inertial range scaling law for second-order

structure functions, known as the Kolmogorov constant C_2, is a universal constant (Praskovsky *et al.* 1993; Sreenivasan 1995; Yeung & Zhou 1997; Mouri *et al.* 2006).

In this paper, we systematically change the fluctuations in the energy input at the large scales and find that this leads to a decrease in the Kolmogorov constant C_2 that can be more than 20 %. An extension of the idea behind Kolmogorov's refined theory provides a model that successfully predicts these changes of the coefficients in the inertial range scaling laws.

We also use structure functions conditioned on the velocity sum to measure the effect of fluctuations of large-scale energy input on small scales. These conditional structure functions are able to identify the effects of fluctuations of the energy input even when the fluctuations are small. The curvature of the second-order conditional structure functions appears to be determined by fluctuations in the energy input in a way similar to the changes in the Kolmogorov constant, but a quantitative understanding of this relationship is not available.

The turbulent flows that have been the focus of most laboratory and simulation work appear to have small enough fluctuations in the energy input that the effects on the second-order Kolmogorov constant are usually negligible. However, in many geophysical flows such as turbulent clouds, the large-scale fluctuations are a dominant feature of the flow. Our measurements show that fluctuations in the energy input at large scales can be determined by measuring the coefficients of the inertial range scaling law or conditional structure functions. This allows small-scale measurements to provide a useful diagnostic of large-scale dynamics. When it is possible to make direct measurements or predictions of the fluctuations in the large-scale energy input, then the models we use here can provide predictions of the inertial range scaling coefficients from the properties of the large scales.

Acknowledgements

REFERENCES

ANTONIA, R. A. & BURATTINI, P. 2006 Approach to the 4/5 law in homogeneous isotropic turbulence. *J. Fluid Mech.* **550**, 175–184.

BATCHELOR, G. K. & TOWNSEND, A. A. 1949 The nature of turbulent motion at large wave-numbers. *Proc. R. Soc. Lond.* A **199**, 238–255.

BLUM, D. B., BEWLEY, G. P., BODENSCHATZ, E., GIBERT, M., GYLFASON, A., MYDLARSKI, L., VOTH, G. A., XU, H. & YEUNG, P. K. 2011 Signatures of non-universal large scales in conditional structure functions from various turbulent flows. *New J. Phys.* **34**, 114020.

BLUM, D. B., KUNWAR, S. B., JOHNSON, J. & VOTH, G. A. 2010 Effects of nonuniversal large scales on conditional structure functions in turbulence. *Phys. Fluids* **22**, 015107.

BOS, W. J. T., CLARK, T. T. & RUBINSTEIN, R. 2007a Small scale response and modelling of periodically forced turbulence. *Phys. Fluids* **19**, 055107.

BOS, W. J. T., SHAO, L. & BERTOGLIO, J.-P. 2007b Spectral imbalance and the normalized dissipation rate of turbulence. *Phys. Fluids* **19**, 045101.

CADOT, O., TITON, J. H. & BONN, D. 2003 Observation of resonances in modulated turbulence. *J. Fluid Mech.* **485**, 161–170.

CHAN, D., STICH, D. & VOTH, G. A. 2007 Real time image compression for high-speed particle tracking. *Rev. Sci. Instrum.* **78**, 023704.

DAVIDSON, P. A. 2004 *Turbulence: An Introduction for Scientists and Engineers*. Oxford University Press.

DONZIS, D. A. & YEUNG, P. K. 2010 Resolution effects and scaling in numerical simulations of passive scalar mixing in turbulence. *Physica* D **239**, 1278–1287.

FRISCH, U. 1995 *Turbulence: The legacy of A. N. Kolmogorov*. Cambridge University Press.

VON DER HEYDT, A., GROSSMANN, S. & LOHSE, D. 2003 Response maxima in modulated turbulence. *Phys. Rev.* E **67**, 046308.

HINZE, J. O. 1959 *Turbulence: An Introduction to its Mechanism and Theory*. McGraw-Hill.

HINZE, J. O. 1975 *Turbulence*, 2nd edn. McGraw-Hill.

ISHIHARA, T., GOTOH, T. & KANEDA, Y. 2009 Study of high-Reynolds number isotropic turbulence by direct numerical simulation. *Annu. Rev. Fluid Mech.* **41**, 165–180.

JIN, X.-L. & XIA, K.-Q. 2008 An experimental study of kicked thermal turbulence. *J. Fluid Mech.* **606**, 133–151.

KANG, H. S. & MENEVEAU, C. 2008 Experimental study of an active grid-generated shearless mixing layer and comparisons with large-eddy simulation. *Phys. Fluids* **20**, 125102.

KOLMOGOROV, A. N. 1941 The local structure of turbulence in incompressible viscous fluid for very large Reynolds numbers. *Dokl. Akad. Nauk SSSR* **30**, 301–305.

KOLMOGOROV, A. N. 1962 A refinement of previous hypotheses concerning the local structure of turbulence in a viscous incompressible fluid at high Reynolds number. *J. Fluid Mech.* **13**, 82–85.

KUCZAJ, A. K., GEURTS, B. J. & LOHSE, D. 2006 Response maxima in time-modulated turbulence: direct numerical simulations. *Europhys. Lett.* **73**, 851–857.

KUCZAJ, A. K., GEURTS, B. J., LOHSE, D & VAN DE WATER, W. 2008 Turbulence modification by periodically modulated scale-dependent forcing. *Comput. Fluids* **37**, 816–824.

LANDAU, L. D. & LIFSCHITZ, E. M. 1944 Fluid Mechanics (in Russian) USSR. (Also 2nd edition, Pergamon Press, 1987).

MI, J. & ANTONIA, R. A. 2001 Effects of large-scale intermittency and mean shear on scaling-range exponents in a turbulent jet. *Phys. Rev.* E **64**, 026302.

MOISY, F., TABELING, P. & WILLAIME, H. 1999 Kolmogorov equation in a fully developed turbulence experiment. *Phys. Rev. Lett.* **82**, 3994–3997.

MONIN, A. S. & YAGLOM, A. M. 1971 *Statistical Fluid Mechanics: Mechanics of Turbulence*. MIT Press.

MOURI, H., TAKAOKA, M., HORI, A. & KAWASHIMA, Y. 2006 On Landau's prediction for large-scale fluctuation of turbulence energy dissipation. *Phys. Fluids* **18**, 015103.

OBUKHOV, A. M. 1962 Some specific features of atmospheric turbulence. *J. Fluid Mech* **13**, 77–81.

POPE, S. B. 2000 *Turbulent Flows*. Cambridge University Press.

PRASKOVSKY, A. A., GLEDZER, E. B., KARYAKIN, M. Y. & ZHOU, Y. 1993 The sweeping decorrelation hypothesis and energy-inertial scale interaction in high Reynolds number flows. *J. Fluid Mech.* **248**, 493–511.

SREENIVASAN, K. R. 1995 On the universality of the Kolmogorov constant. *Phys. Fluids* **7**, 2778–2784.

SREENIVASAN, K. R. & ANTONIA, R. A. 1997 The phenomenology of small-scale turbulence. *Annu. Rev. Fluid Mech.* **29**, 435–472.

SREENIVASAN, K. R. & DHRUVA, B. 1998 Is there scaling in high-Reynolds-number turbulence? *Progr. Theor. Phys.* **130**, 103–120.

SREENIVASAN, K. R. & STOLOVITZKY, G. 1996 Statistical dependence of inertial range properties on large scales in a high-Reynolds-number shear flow. *Phys. Rev. Lett.* **77**, 2218–2221.

VEERAVALLI, S. & WARHAFT, Z. 1989 The shearless turbulent mixing layer. *J. Fluid Mech.* **207**, 191–229.

YEUNG, P. K. & ZHOU, Y. 1997 Universality of the Kolmogorov constant in numerical simulations of turbulence. *Phys. Rev.* E **56**, 1746–1752.